Metallomics

Accepted Manuscript

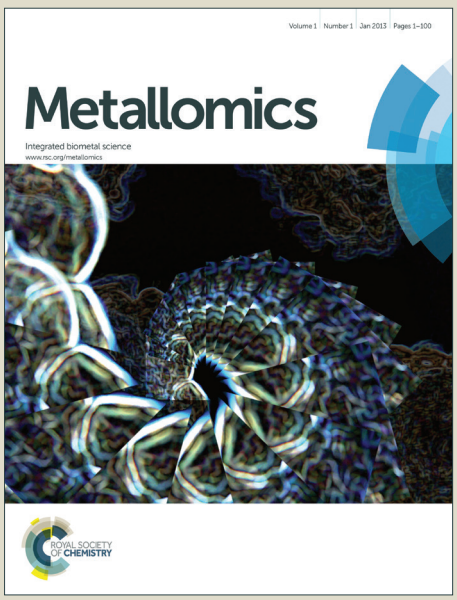

ROYAL SOCIETY OF CHEMISTRY

www.rsc.org/metallomics

On the molecular relationships between high-zinc tolerance and aconitase (Aco1) in *Saccharomyces cerevisiae*

Maria Guirola[#], Elena Jiménez-Martí[#,*] and Silvia Atrian

Dept. de Genètica, Fac. de Biologia, Universitat de Barcelona, Av. Diagonal 643, 08028-Barcelona, Spain

[#] Both authors contributed equally to this work

*Corresponding author:

Departament of Genetics, Faculty of Biology, University of Barcelona, Av. Diagonal 643, 08028 Barcelona, Spain, Tel.: +34934035528; Fax: +34934034420; E-mail: elena.jimenez@ub.edu

Abstract

Zinc is an essential metal for all organisms, as it participates in the structure and/or function of many proteins. However, zinc excess is as deleterious to cells as zinc deficiency. A genome-wide study of the transcriptomic response to high zinc in *S. cerevisiae* performed in our laboratory allowed the identification of a zinc hyper-tolerant deletion mutant (*pif1),* which lacks the Pif1 DNA helicase. Further molecular characterization of this strain phenotype revealed that the lack of Pif1 leads to increased iron accumulation, redistribution of the aconitase protein to mitochondria, and also a loss of aconitase activity, despite of normal Aco1 protein levels being present, probably due to the epistasis in protecting mtDNA between *PIF1* and *ACO1*. The results presented in this work focus now on the characterization of different features related to the Aco1 protein and activity in yeast and the tolerance to high zinc. Hence, multiple phenotypic traits related with metal metabolism, namely Aco1 protein content and activity level, succinate dehydrogenase activity, citrate levels, metal content, BPS influence in cultures, and range of transcription of some iron metabolism related genes, have been analyzed for several strains, some of them constructed to this end, including BY4741, the deletants *pif1*Δ and *aco1*Δ*,* and the *aco1* mutants *aco1*Δ-d4, *aco1*-C448S, *aco1*-R476S and *aco1*-R668S. Overall, lack of Aco1 enzymatic activity in mitochondria, citrate accumulation and lack of activity of [Fe-S] enzymes, *e.g*. succinate dehydrogenase, appear as direct molecular indicators for increased zinc tolerance in *S. cerevisiae*.

Keywords: yeast, *Saccharomyces cerevisiae,* zinc, iron metabolism, aconitase, Pif1, mitochondria, citrate, iron-sulfur center

1. Introduction

Baker's yeast is largely used as a model organism to infer individual gene functions, gene and protein interactions, and regulatory network structures, through various types of molecular biology approaches, ranging from individual assays to high-throughput genome scale experiments. A high degree of conservation of cellular pathways involved in copper, iron and zinc metabolisms, including import, distribution and export mechanisms has been observed between *Saccharomyces cerevisiae* and humans.[1,2] This supports the use of *Saccharomyces cerevisiae* as a model organism to study metal metabolism and associated alterations in eukaryotes. Among trace elements, zinc is present to around 9% of proteins in eukaryotic proteomes,[3] and it has been shown to be an essential metal for almost all living organisms. However, zinc excess or defect is deleterious to the cell, being the control of zinc homeostasis of great importance to ensure a successful life span.

Although yeast mechanisms involved in the response to zinc deficiency have been thoroughly characterized,[4] little is known about the genomic response to zinc surplus. Our previous studies have shown that the lack of Pif1, a DNA helicase located both in nucleus and mitochondria, disrupts zinc and iron homeostasis in yeast, and results in tolerance to high zinc.[5,6] The *pif1*Δ mutant is characterized by increased intracellular iron (total and mitochondrial), diminished ROS formation under zinc surplus, and overexpression of TCA related genes, as *ACO1*.[5,6] Besides, we reported a redistribution of the aconitase protein content in cytosol and mitochondria, and the total abrogation of aconitase activity in *pif1*Δ cells, although Aco1 protein levels remained unaltered. Our observations led to the conclusion that the moonlighting nature of aconitase, as enzyme and mitochondrial nucleoid component, could be in the crossroad of the pleiotropic effect of the *PIF1* deletion, although at that time we were unable to provide further molecular clues for these unexpected observations. Although not directly related to zinc, aconitase is one of the most studied proteins in relation to another metal metabolism, iron, and its regulation in eukaryotes. Aconitase is an enzyme of the tricarboxylic acid cycle (TCA) located mainly in mitochondria, and which contains an iron sulfur [4Fe-4S] cluster essential for enzymatic activity, but not for any other of its functions. In animal organisms, aconitase is also found in the cytosol, where it is known as the iron response protein 1 (Irp1) and binds to the iron-responsive elements (IRE) in the untranslated regions of mRNAs coding for proteins involved in iron metabolism, thus becoming a regulator of the iron homeostasis response.[7] In yeast, aconitase displays also a bi-functional role in the cell, although no IRP-like performance has been described. On the one hand, it is enzymatically active in the TCA cycle catalyzing the interconversion of citrate to isocitrate, while on the other hand it contributes to the mitochondrial DNA (mtDNA) packaging and maintenance, as a component of the mtDNA nucleoids.[8,9] Thus, as in animals, the second role of aconitase is related to nucleic acid binding, and

the homologous residues of the Aco1 protein have been suggested as responsible for either DNA or RNA interaction.[9] It is well known that mutants lacking *ACO1* lose their mtDNA, and that the failure to correctly attach the iron sulfur cluster to the Aco1 scaffold results in a complete loss of the enzymatic activity.[8] Thus, *aco1*Δ mutants present a petite phenotype, while they also exhibit growth problems in non-fermentable carbon sources.[8] Furthermore, the finding that the expression of *ACO1* is under the control of two powerful regulatory pathways: the heme activator protein system (HAP), in cells with an active respiratory metabolism, and the retrograde system (RTG), in cells with compromised or dysfunctional mitochondria, has already suggested that Aco1 could be part of a metabolic mechanism coupling the energy metabolism to mtDNA maintenance.[10]

In the frame of all this information, this study is devoted to unveil molecular relationships between the increased zinc tolerance phenotype and the absence or mutation of the enzyme Aco1. After the thorough analysis of a series of metal-related features of different yeast strains, some of them constructed in this work, we propose that the high citrate levels that are accumulated as a consequence of Aco1 total or partial lack of function in mitochondria, as well as the sensing of altered [Fe-S] assembly or status, may be the key to understand iron accumulation and subsequent high zinc tolerance in yeast cells.

2. Experimental

2.1. Yeast strains and culture conditions

All the yeast strains and mutant constructs used in the present study are described in Table S1. Yeast cells were grown in rich medium (YPD, 1% (w/v) yeast extract, 2% (w/v) peptone and 2% (w/v) glucose). When indicated, cells were grown in synthetic complete (SC) medium containing 0.67% (w/v) yeast nitrogen base, the necessary mixture of amino acids and glucose 2% (w/v) as carbon source. Solid media also contained 2% (w/v) agar. For growth assay experiments in plates, yeast cultures were diluted to the same optical density (OD_{600} ~0.1) from overnight cultures and growth until OD_{600} ~0.4-0.6. Drops of 3 µl of serial dilutions (1:10) were spotted onto YPD-derived plates, which were incubated at 30 ºC for the indicated times. For growth assays in liquid media, yeast cultures were diluted to the same optical density (OD_{600} ~0.1) in different media (supplemented as indicated) from overnight cultures and the growth was monitored by measuring the OD_{600} through 48 h. For metal measurements, BY4741 and all the assayed mutant strains were grown in YPD medium until exponential phase (OD_{600} ~0.6), and growth was resumed in the absence or the presence of 5 mM $ZnCl_2$ for 24 h, when the stationary phase (OD_{600} of 2.5–3.0, depending on the zinc concentration) was reached. Samples containing 40 and 80 units of OD_{600} of cells (for total and mitochondrial metal content, respectively) were taken at the moment of metal addition (t=0) and after 24 h (t=24). For aconitase protein and activity measurements, cells were

grown as described for metal determination, except that 20 and 25 absorbance units were collected for protein quantification and activity assay respectively, and that cells were taken at stationary phase (24 h). All absorbance measurements were made in a Genesys 10uv spectrophotometer (Thermo Scientific).

2.2. Genetic constructions, cloning and site directed mutagenesis

Four Aco1 protein mutants were used in this work. The cDNA for the *aco1*-R476S and *aco1*-R668S site-directed mutants (Aco1 amino acid sequence in Uniprot #P19414), were kindly provided by Dr. Chen (University of Texas, USA).[11] The cDNAs for *aco1*-C448S and *aco1*-Δ*d4* were constructed by mutagenic PCR, as detailed below, using the primers described in Table S2, all of them including *BamHI* and *XhoI* restriction sites at their 5'- and 3'-ends respectively, for cloning purposes. The *ACO1* ORF was amplified by PCR on purified BY4741 genomic DNA using the ACO1-Fwd1 and ACO1-Rv1 primers. A cDNA encoding an *aco1* mutant lacking the entire forth protein domain (*aco1-Δd4*) was also constructed by PCR on BY4741 genomic DNA, using the ACO1-Fwd1 and ACO1-ΔD4-Rv primers. This introduces a stop codon after position 1731 of the coding sequence, thus skipping the last domain of Aco1 (amino acids from 577 to 778 of the protein sequence). In all cases, the PCR reaction conditions were: 1 cycle at 94 ºC for 3 min, 30 cycles at 94 °C for 30 sec, 30 sec at 55 ºC, 1-3 min at 72 ºC and, finally, a 7-min cycle at 72 °C, as suggested by the manufacturer of the Expand Long Template PCR System (Roche). The site-directed-mutant *aco1*-C448S was obtained using the QuikChange Lightning Multi Site-Directed Mutagenesis Kit (Agilent®) on the wild type *ACO1* ORF as template, with the mutagenic ACO1-C448S-Primer. All the cDNAs were cloned into the multicopy expression pVT-U vector[12] for overexpression and into the centromeric pRS316 plasmid[13] for complementation assays. Transformants of the different plasmids were obtained by the lithium acetate method,[14] and they were selected in SC-URA media.

A conditional *aco1* mutant was constructed in a tetracycline-regulatable expression system, kindly provided by Dr. Herrero (Universitat de Lleida, Spain).[15] The promoter-substitution cassette in plasmid pCM225 was employed for replacing the endogenous *ACO1* promoter by the $tetO_7$ promoter in the MML830 strain using the ACO1-tetO7-Fwd and ACO1-tetO7-Rv primers (Table S2). Promoter substitution was checked by PCR using specific primers for amplification of the substitution cassette (Aco1-tetO7-CkFwd and Aco1-tetO7-CkRv), for the amplification of the whole construct (Aco1-tetO7-WhFwd and Aco1-tetO7-WhRv) and for amplification of *ACO1* ORF as control (ACO1-Fwd2 and ACO1-Rv2). PCR conditions were those recommended for the Expand Long Template PCR System (Roche), as detailed before. The *PIF1* ORF was disrupted in this strain (p$tetO_7$-*ACO1*) and also in MML830, by replacing it by the *TRP1* cassette from the pFA-6a-TRP plasmid from Longtine collection.[16] The cassette was amplified by PCR (conditions as before,

annealing at 53 ºC and 1.65 min of elongation) using the primers PIF1-TRP1-disrup Fwd and PIF1-TRP1-disrup Rv (Table S2). Both strains were transformed in order to get a *pif1*Δ in the MML830 background and a conditional double mutant p*tetO*$_7$*-ACO1-pif1*Δ, in the same background (Fig. 1). Transformants were checked by PCR (conditions as before, annealing at 50 ºC and 2.5 min of elongation) using the primers PIF1-TRP1-check Fwd and PIF1-TRP1-check Rv (Table S2). All the constructs used in this work were sequenced using the ABI PRISM Big Dye Terminator v3.1 Cycle Sequencing Kit (Applied Biosystems) in an ABI PRISM 310 automatic sequencer. The mutant construction *aco1*-C448S was sequenced using internal primers (ACO1-C448S-SeqFw and ACO1-C448S-SeqRv), while all the other constructions were sequenced from the M13 primers.

2.3. Total and mitochondrial metal content measurement

Cellular metal content was measured by inductively coupled plasma-atomic emission MS (ICP-OES) in a Polyscan 61E equipment (Thermo Jarrell Ash), as described.[6] Mitochondria were isolated using a yeast mitochondria isolation kit (MITOISO3®, Sigma–Aldrich), as in our *pif1*Δ analysis, and the quality of the mitochondria preparation was assessed as described therein.[5] Mitochondrial metal content was measured by inductively coupled plasma mass spectrophotometry (ICP-MS) in an Eland 6000 equipment (PerkinElmer). Total metal content was normalized by dry cell weight, while mitochondrial metal content was normalized by total mitochondrial protein, determined by the Quick StartTM Bradford protein assay kit (Bio-Rad), with BSA as standard. Statistical analysis was performed following the Newman-Keuls multiple comparison test.

2.4. Measurement of aconitase activity and protein, and citrate content

Aconitase activity and protein levels were measured in total cell extracts from 25-absorbance units of cells. Aconitase activity was determined as originally reported [17,18] with the modifications already described.[6] The aconitase protein content was measured by a quantitative ELISA as described, through a standard calibration curve of porcine heart aconitase (Sigma–Aldrich) starting at 4 μg/ml.[5] In all cases, statistical analyses were performed following the Newman-Keuls multiple comparison test. The total protein content was determined as above. For citrate measurement, aliquots of 60-absorbance units of cells were taken at two different OD_{600} points (0.4 and 2) and treated as described.[19] The citrate content was measured from 150 µl of cell extract by using the Citric Acid Analysis Kit ® (Roche).[20]

2.5. Measurement of succinate dehydrogenase activity

The succinate dehydrogenase activity was measured as reported,[21] but for the following differences. Cells were inoculated in YPD and grown overnight. Then, they were diluted in fresh medium at an OD_{600}~0.1 and grown to ~0.4. In that moment, $3 \cdot 10^8$ cells were harvested by

centrifugation (2,100 x*g*, 10 min), and washed twice in Ringer's solution. Cells were subsequently diluted in 1 ml of Ringer's solution and 0.1% Triton X-100 and incubated at 30 ºC for 15 min, and they were centrifuged again in the same conditions. After that, 0.3 ml of 0.5 M substrate dilution (sodium succinate or glucose as a negative control); 3 ml of a solution containing 0.68 mM blue tetrazolium (BT) salt, 50 mM sodium azide, 5mM EDTA and 100 mM N,N-dimetylformamide; and 1 small crystal of phenazine methosulphate (PMS) were added to the pellet, and incubated at 37 ºC for 1 hour. The reaction was stopped by addition of 0.4 ml of 37% formaldehyde, and centrifuged as before. Finally, the pellet was extracted once with 3 ml and twice with 2 ml of DMSO, and centrifuged under the same conditions. The supernatants were collected together and 1 ml was used to measure the absorbance at 540 nm. To quantify the BT-formazan in each sample, a standard curve using BT salts was also calculated. Serial dilutions from 0.02 to 0.68 mM BT salts in a final volume of 1 ml were incubated with 40 µl of 80% hydrazine hydrate for 30 min at 100 ºC. Formazan crystals were diluted in 7 ml of DMSO and 1 ml was used to measure the absorbance at 540 nm.

2.6. RNA extraction and semi-quantitative RT-PCR

For RNA purification, yeasts were grown in 150-ml YPD cultures to mid-log (OD_{600} ~0.4) and steady-state phase (OD_{600} ~2), collected by centrifugation, frozen in liquid nitrogen and stored at –80 °C. Cell pellets were resuspended in 0.5 ml of LETS buffer (0.1 M LiCl, 0.01 M EDTA, 0.01 M Tris-HCl (pH 7.4), 0.2% (w/v) SDS). Cells were disrupted using a TissueLyser II (Retsch) by 2 pulses at a frequency of 30 s^{-1}, following the addition of 0.5 ml of 425–600 micron glass beads and 0.5 ml of saturated phenol (pH 4.3). After one extraction with phenol:chloroform:isoamyl alcohol (125:24:1), RNA was precipitated with one volume of 5 M lithium chloride and stored at –80 °C for at least 2 h. The precipitated RNA was washed with 70% ethanol and resuspended in RNase-free water. RNA was quantified by measuring the absorbance at 260 nm. Agarose gel electrophoresis in TAE buffer (0.04 M Tris-acetate, 0.001 M EDTA pH 8.0) was used to check the quality and integrity of the RNAs. The expression levels of the selected genes (Table S3) were analyzed by semi-quantitative reverse transcription-polymerase chain reaction (RT-PCR). For cDNA preparation, 10 µg of RNA were incubated with 1µl of RQ1 DNase (Promega) in a total volume of 56.1 µl at 37 ºC for 30 min and the reaction was stopped by incubation at 65 ºC for 10 min. Then, 1 µg of RNA from the previous preparation was incubated with 1 µl of oligo $(dT)_{18}$ (Roche) and 2 µl of random hexamers in a final volume of 13 µl for 10 min at 65 ºC, and then placed in ice. Afterwards, 4 µl of 5 × RT buffer, 2 µl of dNTPs (10 mM each), 0.5 µl of RNAI (Roche) and 0.5 µl Retrotranscriptase (200 U) were added and a first incubation at 25 °C was carried out for 10 min, followed by a second incubation at 55 °C for 30 min. Finally, the reaction was stopped by

incubating 5 min at 85 ºC, and the samples were stored at -80 ºC. 0.5 µL of the resulting cDNA, was used for a PCR reaction to amplify each specific genes. This reaction was performed in a final volume of 25 µl containing the specific primers listed in Table 3, under the following conditions: 1 cycle at 94 °C for 3 min, 20–25 cycles at 94 °C for 1 min, 1 min at the optimal primer hybridization temperature in each case, 1-2 min at 72 °C and, finally, a 10-min cycle at 72 °C. *ACT1*, which encodes a structural protein involved in housekeeping functions (cell polarization, endocytosis, and other cytoskeletal roles) was used for data normalization, as commonly applied by other authors.[22,23]

3. Results

3.1. Lack of the *ACO1* gene results in increased zinc tolerance

The link between the lack of Aco1 activity and zinc resistance in yeast was patently supported by the increased survival to zinc surplus of *aco1Δ* cells (Fig. 2A), even slightly more pronounced than that of the zinc-resistant *pif1*Δ strain, which keeps normal, but redistributed, Aco1 protein levels.[5] To corroborate this relationship, a conditional mutant, in which *ACO1* transcription was under control of the $tetO_7$ switchable promoter, was constructed, so that doxycycline switched off *ACO1* transcription. Under no zinc supplementation, doxycycline provoked only a slight growth defect, compatible with the lack of aconitase activity, but when cells were grown on 5 mM $ZnCl_2$-YPD, the silencing of *ACO1* clearly increased their zinc tolerance (Fig. 2B). Therefore, hampering *ACO1* expression yielded the same effect as the absence of *ACO1* from the genome. Experiments using the constructs shown in Fig. 1 revealed that the relative influence of Pif1 and Aco1 on zinc tolerance in MML830 was different than in the BY4741 background (Fig. 3). Hence, the zinc hypertolerance of MML830-*pif1*Δ was more pronounced than that of the BY4741-*pif1*Δ deletant, while the absence of Aco1 in MML830 only supposed a slight increase of the tolerance. It is worth noting that the double absence of both proteins rendered cells only slightly more tolerant than those where *ACO1* expression had been silenced, and far less tolerant than MML830-*pif1*Δ.

3.2. Enzymatic dysfunction of *ACO1* entails zinc tolerance

Next, we aimed at testing the influence of the different Aco1 moonlighting functions[8] in zinc tolerance, using the mutants described below. *aco1*-R476S and *aco1*-R668S encode two Aco1 proteins with reduced DNA binding ability (50% and 20%, respectively),[11] but enzymatically active (75% and 87%, respectively; our data in Fig. 4), concordantly with the features of their homologous pig aconitase mutants.[24] Aco1-C448S is a protein with unaltered DNA-binding capacity,[11] but which is a dead enzyme since Cys 448 is essential for coordination of its [Fe-S] center.[25] Finally, Aco1-Δd4 is a truncated protein lacking its entire 4th domain that was recently characterized as a dual targeting signal between mitochondria and cytosol, necessary for both import into

mitochondria and cytoplasm relocation.[11,26] The Aco1-Δd4 protein is enzymatically inactive because several substrate binding residues map in the Aco1 4th domain,[25] and it almost lacks any DNA binding capacity (10%).[11] Cloning of *aco1*-C448S and *aco1*-Δd4 into the pRS316 centromeric plasmid provided the *aco1*Δ-complemented cells with one gene copy per genome, this is a gene dose comparable to that of the genome-integrated *aco1*-R476S and *aco1*-R668S mutants.

All these strains were assayed for Zn tolerance, together with BY4741 and *aco1*Δ as controls (Fig. 4A). The tolerance of *aco1*-C448S and *aco1*-Δd4 was similar to that observed for *aco1*Δ, which confirmed the correlation between total lack of aconitase activity and Zn hypertolerance. The *aco1*-R476S cells exhibited Zn sensitivity parallel to that of BY4741, consistent with their Aco1 activity, although partial (75%). However, the high Zn resistance of *aco1*-R668S resulted discordant with our hypothesis, since it grew well at even 7 mM $ZnCl_2$, despite exhibiting substantial Aco1 activity (87%). To further analyze these two mutants, we checked their capacity to grow in non-fermentable media (YPD-glycerol and YPD-ethanol), as indicative of their mtDNA stability (Fig. S2). While *aco1*-R476S was perfectly able to exhibit both fermentative and respiratory metabolism, like the wild type strain, the highly impaired growth of the *aco1*-R668S cells on non-fermentable carbon sources indicated a high instability of their mtDNA. Finally, the measurement of Aco1 protein and activity levels in isolated mitochondria of BY4741, *aco1*-R476S and *aco1*-R668S cells indicated that while Aco1 appears to be present roughly at the same amount in the mitochondria of the three types of cells, there is a clear deficiency of Aco1 enzymatic activity in the *aco1*-R668S mitochondrial preparations (Fig. S2).

3.3. Aco1 protein content and enzymatic activity are altered in the *ACO1* mutants

Both the total aconitase activity and Aco1 protein content was measured in cells of all the studied strains grown in standard and in zinc-supplemented cultures (Fig. 5). When grown in normal YPD, the BY4741 and *aco1*Δ strains, used as positive and negative controls, yielded results expected from their genotype, *i.e.* normal and null Aco1 activity and protein, respectively, while *pif1*Δ exhibited wild type-like Aco1 levels, but totally abolished aconitase activity, as previously reported.[5] The practically dead Aco1-Δd4 and Aco1-C448S enzymes yielded similar data. Slightly different results were obtained for *aco1*-R476S and *aco1*-R668S. Surprisingly, the *aco1*-R668S cells exhibited Aco1 activity comparable to that of BY4741 cells, and its Aco1 protein content was higher than for the rest of strains ($P<0.05$), whereas *aco1*-R476S produced Aco1-R476S levels comparable to those in *aco1*-Δd4, *pif1*Δ and *aco1*-C448S. In the *pif1*Δ, *aco1*Δ, *aco1*-Δd4 and *aco1*-C448S strains, the aconitase activity:aconitase protein ratio was close to zero, being all these Zn-hypertolerant strains (Fig. 4A). On the other hand, BY4741 and *aco1*-R476S exhibited an activity/protein ratio that was close to 0.04, which could be assimilated to normal zinc sensibility.

For the *aco1*-R668S, the ratio was markedly lower than for *aco1*-R476S, but it is worth remembering that very low Aco1 activity was detected in the mitochondria of these cells (Fig. S2). This suggests that zinc tolerance could be linked to the Aco1 activity in mitochondria. The reduction of the Aco1 activity upon zinc treatment was evident in all Aco1-active strains (BY4741, *aco1*-R476S and *aco1*-R668S), in agreement with data in the literature[27] and our previous results for the wild type strain.[5] Therefore, the increased Aco1 synthesis in the *aco1*-R668S mutants could result from an attempt to compensate for the absence of mitochondrial Aco1 activity in normal cultures, as well as the inhibition caused by the zinc overload. The opposite effect was observed in the *pif1*Δ strain, where both the Aco1 activity and protein levels increased when growing on zinc supplementation, a phenomenon that had been interpreted before for this genetic background on the basis of the forced dual role of Aco1 as enzyme and mtDNA protective agent.[8]

3.4. Overexpression of *ACO1* in *pif1*Δ and *aco1*Δ cells rescues wild type zinc tolerance

Our so-far considered hypothesis predicted that ACO1 overexpression in Aco1-deficient cells would revert their Zn hypertolerance phenotype to BY4741 zinc sensitivity levels. To test it, we assayed the Zn tolerance of *aco1*Δ and *pif1*Δ cells transformed with the multicopy expression construct *ACO1*/pVT-U, as well as with the void pVT-U vector as control. The Aco1 protein and activity levels were concurrently determined. Results first show that in the *aco1*Δ background, exogenous ACO1 overexpression restored both Aco1 protein and activity values to those exhibited by the wild type strain, while in the *pif1*Δ transformants, the Aco1 protein content was increased, with a concomitant recovery of the aconitase activity (Fig. 6 A,B). Coincidently with the recovery of aconitase activity, the zinc tolerance of the transformed *aco1*Δ + *ACO1*/pVT-U and *pif1*Δ + *ACO1*/pVT-U strains significantly decreased (Fig. 6C). The growth on SC medium guaranteed that no plasmid loss occurred during the experiments, being the BY4741 and derived *aco1Δ* and *pif1Δ* strains auxotrophic for uracil. The results on SC-Ura-Zn cultures not only were coincident with those on YPD-Zn, but also showed more clearly that the presence of the cloned *ACO1* gene always diminished the Zn tolerance regarding the respective "void strain" (either *aco1Δ* or *pif1*Δ). It is worth noting that the presence of the non-recombinant pVT-U plasmid did alter neither the Aco1 activity nor protein levels of any of the transformed host cells (*cf.* Fig. 6A,B).

3.5. Citrate content is altered in *pif1*Δ and *aco1*Δ mutants

Citrate accumulation provoked by a blocked TCA cycle was considered as a feasible link between decreased aconitase activity and metal ion homeostasis alterations in yeast cells. Citrate, the TCA aconitase substrate, is a well-known zinc and iron chelator, acting on the free-metal cell pools.[19,27,28] Therefore, we proceeded to investigate if abnormally high citrate levels were present in all our strains. The corresponding results revealed that both the *aco1*Δ and *pif1*Δ cells accumulated

approximately two-fold citrate levels regarding the wild type BY4741 strain, in exponentially growing cells (Fig. 7). Increased citrate is concordant with the interruption of the TCA cycle, as reported by other authors in different genetic background and growth conditions (*e.g.* MMY001 strain in galactose[19]). The *aco1*-R476S strain, also zinc-sensible, exhibited low citrate, very much alike those of wild type cells, which was concordant with their partial aconitase activity. Most significantly, the zinc hypertolerant mutants (*aco1*-Δd4, *aco1*-C448S and *aco1*-R668S) were all characterized by the highest citrate content among all strains. These results suggest a clear citrate-level threshold that splits Zn-sensitive from Zn-tolerant genotypes.

3.6. Zinc and iron homeostasis are disrupted in *ACO1* mutants

Metal homeostasis disruption was tested in our set of yeast strains through the measurement of total cell and mitochondrial Zn and Fe contents of cells grown in normal and in Zn-supplemented YPD (Fig. 8). When no zinc had been added, no significant differences could be detected for either the total or the mitochondrial zinc content, between wild type and *pif1*Δ cells. Contrarily, total zinc content increased when cells of these two strains grew in zinc-YPD medium, but mitochondrial zinc was dramatically increased only in *pif1*Δ (reaching 7.38 ng/mg of protein), compared to 2.88 ng Zn/mg of protein in wild type BY4741 (Fig. 8A), as observed before.[5] Remarkably, all the *aco1* mutants shared an enormous accumulation of intracellular zinc (between x10 and x15 the values of BY4741) after 24-h growth in Zn-YPD, a feature that, however, appeared not to be related to their respective zinc tolerance capacity. Contrarily, resistance to high Zn seemed to be closely related to the hyper-accumulation of zinc in mitochondria, as otherwise observed for *pif1*Δ, with the difference that mitochondrial zinc hyper-accumulation was much more accentuated for the *aco1* mutants that were Zn-resistant (Fig. 8B). Concordantly, the zinc sensitive *aco1*-R476S cells did not significantly increase their mitochondrial zinc, while all the clearly Zn hypertolerant mutants accumulated between x10 and x20 Zn levels in mitochondria, when compared to BY4741.

Regarding their iron content, all the *aco1* mutants were characterized by high total Fe accumulation, which was worth highlighting for *aco1*Δ, *aco1*-Δ*d4* and *aco1*-C448S grown for 24 h in non-supplemented medium (Fe content of 3.525, 3.786, 3.606 mg Fe/g dry cells, respectively, Fig. 8C). Remarkably, these three strains synthesize completely inactive Aco1. Therefore, our results suggest that the absence of Aco1 enzymatic activity leads to an increased capacity for total iron accumulation, which, nevertheless, is abrogated by a surplus of Zn present in the medium. Partially active Aco1 mutants exhibit total Fe levels of approximately half the content of the Aco1-inactive strains, except *aco1*-R668S, with Fe contents similar to those of *aco1*-R476S. For mitochondrial iron, no major differences were detected among the *aco1* strains, and between these and the wild type BY4741 reference (Fig. 8D), except for the *aco1*-C448S and *aco1*-R668S cells, which exhibited unusually high mitochondrial Fe after 24-h growth under Zn-supplementation.

Finally, it is worth noting that our results reproduced the extraordinary high mitochondrial Fe contents that characterize the exponential growth of *pif1*Δ,[5] this somehow validating the set of measurements presented for all the other analyzed strains. Consequently, it is clear that no uniform relationship can be observed between zinc hypertolerance and neither total nor mitochondrial Fe accumulation for *aco1* mutant cells.

All these results suggested a metal (zinc and iron) accumulation pattern significantly divergent for the *pif1*Δ and *aco1* deletants, independently of their zinc tolerance phenotype. Further evidence that Zn and Fe metabolisms follow different patterns in these two mutants was provided by the determination of the effect that BPS (bathophenanthroline disulfonic acid), a cellular iron chelator, caused in their growth both in non- and Zn-supplemented YPD. Chelating iron reduced the Zn hypertolerance of both the wild type and the *pif1*Δ cells, but had no detectable effect in the *aco1*Δ cultures, which grew similarly to those without BPS (Fig. S1). These results show that, while iron availability can be considered a key factor determining zinc tolerance in wild-type and *pif1*Δ cells,[5] this is not the case for the *aco1* background, an observation that is in close agreement with the different metal accumulation patterns previously shown.

3.7. Iron metabolon was upregulated in *aco1*Δ and *pif1*Δ mutants

The expression levels of a set of genes (Table S3) differently associated with iron uptake and transport[29] was evaluated in the BY4741, *aco1*Δ and *pif1*Δ backgrounds, to investigate if the iron metabolon was disrupted in these cells. Firstly, it is worth noting that expression of *AFT1* was not detected in any cell type, which is compatible with the activation of the main iron-responding transcription factor by compartment re-localization and not expression induction,[30] as described for *pif1*Δ.[5] However, unlike in this strain, the transcription of genes related with iron-siderophore transport (*ARN1*, *FIT2* and *FIT3*) remained unaltered in *aco1*Δ cells in relation to BY4741 (Fig. 9). On the contrary, the expression of the genes encoding the high affinity Fe transporters *FTR1*, *FET3* and *FET5* resulted increased in both mutant strains, although under a differential pattern. Hence, while in *pif1*Δ, major expression involves *FET3* in exponential and *FTR1* in stationary growing cells, in *aco1*Δ major transcription activation would occur for *FTR1* in exponentially growing cells. In the case of genes related to intracellular iron trafficking (the vacuolar *CCC1* and the mitochondrial *MRS3* and *MRS4* transporters), an increased expression was observed in both mutants, being more significant for *aco1*Δ than for *pif1*Δ, and in exponential than in stationary growth (Fig. 9), when, strikingly, transcription of these genes was almost silenced in *pif1*Δ. Overall, these results are consistent with an altered iron homeostasis, and as will be discussed below, they are in accordance with the iron levels reported in the previous section of this work.

3.8. Succinate dehydrogenase activity is altered in *pif1*Δ and *aco1* mutants

Succinate dehydrogenase (or succinate-coenzyme Q reductase, SDH) is, like Aco1, a mitochondrial [Fe-S] enzyme of the TCA cycle, and it is generally used to evaluate the state of [Fe-S] assembly and metabolism in cells. Since mitochondrial [Fe-S] cluster biogenesis was proposed as an indicator of the cell iron status, and thus a switch for the iron homeostasis machinery,[31,32] we determined the levels of SDH activity in all our strains, to assess if there was any correlation with their tolerance to high zinc. Unexpectedly, the *aco1*-R476S cells showed approximately an x1.5 fold increase in SDH activity in relation to BY4741 (wild type), and it is worth remembering that these two strains exhibit a parallel high-zinc sensitivity (Fig. 10). On the contrary, all the remaining Aco1 mutants were characterized by SDH activity levels lower than those of BY4741, ranging from 40-50% for *aco1*-Δd4, *aco1*-C448S and *aco1*-C668S, to less than 10 % for *aco1*Δ and *pif1*Δ (Fig. 10). Here again, the difference between zinc-tolerance and zinc-sensitivity seems to rely on a threshold-effect basis. A close relation between SDH activity, Aco1 activity in mitochondria, and Aco1 and Pif1 protein presence is later discussed.

4. Discussion

Abnormal zinc homeostasis causes a variety of health problems in humans that include growth retardation, immunodeficiency, hypogonadism, and neuronal and sensory dysfunctions.[33] Therefore, the correct understanding of metal metabolism regulation and networks is a most interesting field in order to unveil the molecular basis of metal-related human pathologies, and yeast is the most common model used for this kind of studies. Our previous characterization of the yeast deletant for the Pif1 nuclear and mitochrondrial DNA helicase revealed that *pif1*Δ cells were highly tolerant to zinc and that they exhibited a disrupted zinc and iron homeostasis mainly owing to iron accumulation in mitochondria. Unexpected results pointed to aconitase as a key player of the *pif1*Δ phenotype, since *pif1*Δ cells lacked Aco1 activity while maintaining normal levels of the protein, something that was confirmed by the increased zinc tolerance exhibited by the *aco1*Δ deletants.[5,6] As shown now in this work, Zn hypertolerance is independent of the molecular causes leading to the absence of Aco1 activity in cells, since either direct gene deletion (*aco1*Δ), indirect gene epistasis (*pif1*Δ) or promotor silencing (*tetO$_7$-ACO1)* lead to the same phenotypic effect. Contrarily, it is worth noting that the degree of Zn tolerance is dependent on the genetic strain background, since in MML830 (a W303 derivative) and BY4741 cells the absence of Pif1 or Aco1 does not yield comparable results. Nevertheless, *ACO1* exogenous expression in both *pif1*Δ and *aco1*Δ cells always results in the suppression of their Zn hypertolerance, in parallel to the restoration of aconitase protein and activity levels close to those of wild type cells.

The consideration of several features of the set of *aco1* mutants analyzed in this study sheds further light into the relationship between aconitase and zinc tolerance. Hence, although it remains true that all the aconitase inactive strains (*pif1*Δ, *aco1*Δ, *aco1*-Δd4, and *aco1*-C448S) are Zn hypertolerant, the partially-active strains pose an apparent paradox, because while *aco1*-R476S exhibits a Zn sensitivity similar to that of BY4741 (as expected for a *functional-aconitase strain*), *aco1*-R668S clearly tolerates high Zn (Fig. 4). However, *aco1*-R668S exhibits a patently low mitochondrial Aco1 activity, which groups it with the *fully-dead* Aco1 strains. No direct evidence apparently links a defective Aco1-mtDNA binding capacity with the high zinc tolerance phenotype. However, more conclusive hints were provided by high cell citrate content and impaired SDH activity, both indicators unambiguously correlating with high Zn hypertolerance (*cf*. Fig. 7 and 10, respectively). Cell citrate can accumulate up to 10x levels[19] due to the TCA cycle interruption caused by Aco1 malfunction, and it has also been reported that *ACO1* overexpression effectively changes the citric acid production rate.[34] Citrate chelates divalent cations and it has complex functions in metal homeostasis pathways, precisely about iron and zinc.[28,35,36,37,38] In yeast, citrate chelation acts on the labile iron pool, which is a key switch for the activation/silencing of the iron import/export and translocation mechanisms that regulate the iron status in cells. [39] Besides, the activity of SDH is widely accepted as an indicator of the [Fe-S] cluster cell status, another activation signal of the iron import machinery.[32] Consequently, high Zn tolerance seems to be connected to low-iron-like SOS signals: a decreased labile iron pool and an abnormal [Fe-S] cluster status. In another scenario, the capacity of citrate to act as zinc chelator was broadly analyzed in human prostate epithelia cells, where it has been shown to be responsible for their extraordinary zinc buffering and accumulation capacity, and in turn for the inhibition of their aconitase activity.[27,40,41,42] Although with the current data it can not be disregarded that zinc chelation by high citrate could be one among different molecular events converging into a Zn-hypertolerance phenotype, this would be hardly applicable to all the yeast mutants analyzed in this work. Hence, cellular and mitochondrial zinc contents do not always directly correlate with citrate levels, and ultimately with zinc tolerance (Fig. S3 and S4). Although, citrate significantly accumulates to high levels in yeast vacuoles,[43] which is the major zinc storage compartment in yeast cells,[44] *S. cerevisiae* independently regulates mitochondrial and vacuolar zinc, so that phenomena involving vacuolar zinc deposits may not directly influence mitochondrial-related events.

The relationship between the characterized parameters and the Zn resistance of each analyzed yeast genotype is better understood by the comprehensive consideration of all the results obtained for each individual Aco1 mutant. Hence, the *aco1*Δ deletants, lacking both protein and activity, show high-Zn tolerance, citrate accumulation and SDH inhibition, and they are capable to hyper-accumulate both total and mitochondrial Zn, without harmful consequences, after growing in Zn-

supplemented medium. Therefore, they exhibit a pattern of metal (Zn and Fe) accumulation significantly different to that of *pif1*Δ, where Zn levels remained close to those of wild type cells in the same conditions.[5] On the other hand, the increased Fe accumulation detected in *aco1*Δ cells would be located in the cytosol, since mitochondrial Fe remains at similar levels than in wild type cells. The same analysis is valid for *aco1*-Δd4, which shows exactly the same features than *aco1*Δ for all the analyzed parameters. In aco1-C448S, one of the Cys responsible for [Fe-S] coordination has been substituted so that the protein is enzymatically-dead. Surprisingly, the corresponding strain, although also Zn hypertolerant and able to accumulate total Zn and Fe similarly to *aco1*Δ and *aco1*-Δd4, exhibits particular mitochondrial metal contents, with abnormally high iron levels instead of increased zinc. This supports the hypothesis that specifically disrupting the correct [Fe-S] assembly to mitochondrial Aco1 has a direct effect on iron accumulation in this organelle. In *aco1*-R476S, substrate (*i.e.* citrate) interaction is disturbed by the amino acid substitution located in the substrate-binding pocket. Nevertheless, the partial activity retained by this enzyme entails no phenotypic effect regarding citrate accumulation, SDH activity, and consequently Zn resistance, thus in all aspects behaving as the BY4741 strain. The unique difference with the wild type cells lies in an increased accumulation capacity for total Zn and Fe, although significantly not for mitochondrial metal ions. Finally, *aco1*-R668S appeared as a paradoxical strain, because despite also rendering Aco1 activity in total cell homogenates, it exhibited a Zn-resistance similar to that of *aco1*Δ, and coincidently, it also showed increased citrate levels and SDH inhibition, like all the Zn hypertolerant strains. Although the Aco1 activity/protein ratio is slightly lower than for the non-tolerant strains (BY4741 and *aco1*-R476S), this seems not enough to justify a threshold effect determining Zn-tolerance. Definite clues to understand the *aco1*-R668S phenotype could be the almost complete lack of Aco1 activity in their mitochondria, and their incapacity to grow in non-fermentable carbon sources (Fig. S2). Since Aco1 protein levels in mitochondria appear equivalent to those of wild type cells, it may be assumed that the Aco1-R668S protein is present and active in cell cytoplasm, but it becomes inactive inside mitochondria. Mitochondrial Zn content in *aco1*-R668S is extraordinarily high if compared with the other point mutants, while these cells accumulate mitochondrial Fe as much as *aco1*-C448S does. Therefore, it is feasible to hypothesize that in *aco1*-R668S mitochondria, Zn accumulation could affect the correct [Fe-S] cluster assembly, inactivating the enzyme, and ultimately leading to the high mitochondrial iron accumulation measured for these cells. In yeast Aco1, the 668th residue is located in the 4th domain of the protein, and it is supposed to act both on substrate and in nucleic acid binding, as deduced from comparison with the R780 residue in the homologous mammalian enzyme.[45] Concordantly, further support for Aco1 malfunction in *aco1*-R668S cells comes from the observation that they do not grow in non-

fermentable media (YPD-glycerol or -ethanol), contrarily to the other partial-active mutant *aco1*-R476S.

5. Conclusions

From all the analyzed factors, it can be concluded that in yeast, high-zinc tolerance is linked to absence of Aco1 enzymatic activity in mitochondria, incapacity of Aco1 to stabilize the mtDNA, high citrate cell content and impaired SDH activity. We hypothesize that the lack of Aco1 activity in mitochondria, caused either by the absence of protein or by an inactive Aco1 form, would lead to two non-excluding consequences: Zn accumulation and the triggering of the low-iron emergency signals through the chelation of the free iron pool by citrate and/or the disruption of the correct [Fe-S] status. As a consequence, iron import to the cell would be enhanced. The increased mRNA levels of some iron importers, including components of the high affinity iron transporter system through plasma and internal membranes (Fet3, Fet5 and Ftr1), vacuolar importers (Ccc1), and most significantly, mitochondrial iron importers (such as Mrs3 and Mrs4) clearly support this hypothesis. Siderophore transporter gene transcription is not increased in the *aco1*Δ mutant. The iron accumulation pattern of *aco1* mutants and *pif1*Δ is different not only quantitatively, but mainly in cellular distribution. Even though, it can be concluded that besides Zn accumulation, total iron increase is also one of the clues to understand the zinc tolerance in both genotypes. This increased iron level could perform two advantageous functions. On the one hand, it may trigger an early oxidative stress response that is beneficial to resist the ulterior zinc-induced oxidative stress, as previously shown for *pif1*Δ. On the other hand, high iron may preclude inhibitory Zn/Fe substitution in both [Fe-S] and heme groups, which has been claimed as another molecular reason for the toxic effect of high zinc concentrations. Overall, this work is a clear example of cellular integration, since it demonstrates how the cell controls and connects different processes relevant for life, as energy and metal metabolism, mtDNA maintenance and oxidative stress response, to finally balance a successful lifespan even in adverse conditions.

Acknowledgements- This work was supported by the Ministerio de Ciencia y Competitividad, Spain, grants BIO2009-12513-C02-01 and BIO2012-39682-C02-01 to S. A. The receipt of FEDER funds is knowledged. The authors are members of the "Grup de Recerca Consolidat" de la Generalitat de Catalunya ref. 2009SGR-1457. MG was a recipient of a "Ministerio de Asuntos Exteriores y de Cooperación-Agencia Española de cooperación" fellowship. We thank Dr. Chen and Dr. Herrero for the respective kind supply of plasmids and yeast strains used in this work; and also Dr. Ariño for fruitful discussion of some results. We also thank CCiT-UB (Centres Científics i Tecnològics de la Universitat de Barcelona) for allocating DNA sequencing time and for the metal measurement equipment (ICP-OES and ICP-MS).

FIGURE LEGENDS

Figure 1. Schematic representation of the constructs of conditional promoter strains. Four gene combinations of the *ACO1* and *PIF1* ORFs in the genome of MML830 strain are presented. **A**. The wild type ORFs in the parental MML830 strain. **B**. In MML830, the *PIF1* ORF was replaced by the *TRP1* ORF cassette, this yielding an *ACO1-pif1*Δ-like genotype. **C**. In MML830, the *ACO1* promoter was replaced by the doxycycline-conditional promoter $tetO_7$; thus, in the absence of doxycycline, *ACO1* is expressed as in the wild type strain, while in the presence of the antibiotic, the $tetO_7$ promoter switches off the expression of *ACO1*, yielding an *aco1*Δlike genotype. **D**. The *PIF1* replacement by the *TRP1* cassette was performed in the p$tetO_7$-*ACO1* strain, which renders a *pif1*Δ-like mutant when the promoter is on, and a double mutant *aco1*Δ-*pif1*Δ-like, when the promoter is off.

Figure 2. Effect of high zinc levels in different strains. **A**. BY4741, *aco1*Δ and *pif1*Δstrains were grown in YPD medium overnight at 30 ºC and then diluted in fresh YPD medium to an OD_{600} of 0.1. Cultures were grown to an exponential phase (OD_{600} 0.3-0.5) and were then diluted and spotted into YPD and YPD + 5mM $ZnCl_2$ plates. They were allowed to grow for 72h. **B**. MML830 and p$tetO_7$-*ACO1* strains were grown in YPD medium overnight at 30 ºC and the diluted in fresh YPD medium supplemented with 5-µg/ml doxycycline to an OD_{600} of 0.1. Cultures were grown to an exponential phase (OD_{600} 0.3-0.5) and were then diluted, spotted (3 µl) into YPD + 5µg/ml doxycycline and YPD + 5 mM $ZnCl_2$+ 5µg/ml doxycycline plates, and allowed to grow for 48h.

Figure 3. Effect of high zinc levels in the MML830 mutant strains. MML830, *pif1*Δ (MML830); p$tetO_7$-*aco1*Δ (MML830) and p$tetO_7$-*aco1-pif1*Δ(MML830) strains were grown in YPD medium overnight at 30 ºC and then diluted in fresh YPD medium supplemented with 10 µg/ml doxycycline to an OD_{600} of 0.1. Cultures were grown to an exponential phase (OD_{600} 0.3-0.5) and then were diluted and spotted into YPD, YPD + 10 µg/ml doxycycline (Doxy), YPD + 5mM $ZnCl_2$ and YPD + 5 mM $ZnCl_2$ + 10 µg/ml doxycycline plates. They were allowed to grow for 72h.

Figure 4. Effect of high zinc levels in the growth of different *aco1* mutants. Zinc tolerance was analysed in the BY4741 and *aco1*Δ strain, as well as in *aco1* mutants with impaired enzymatic activity (*aco1*-C448S), DNA binding capacity (*aco1*-R476S and *aco1*-R668S), or both (*aco1*-Δ*d4*), as indicated in the table. All strains were grown in YPD medium overnight at 30 ºC and then diluted in fresh YPD medium to an OD_{600} of 0.1. Cultures were grown to an exponential phase (OD_{600} 0.3-

0.5) and then were diluted and spotted into YPD or YPD + 7mM $ZnCl_2$. They were allowed to grow for 72h. Data on DNA-binding capacity and *in vivo* mtDNA maintenance are from ref. 11.

Figure 5. Effect of *aco1* mutations on aconitase content and activity. **A**. Aconitase activity and (**B**) Aco1 protein content were measured in all the *aco1* and *pif1*Δ mutants. Cells were grown in YPD medium overnight at 30 ºC and diluted in fresh YPD medium to an OD600 of 0.1. They were subsequently grown to an OD600 ~0.4 (t_0). Then the culture was divided into two parts, and one of them was supplemented with 5 mM $ZnCl_2$. Both cultures were grown for 24 hours and t_{24} (white bars) and t_{24+Zn} (black bars) and then cells were collected. **C**. The ratio between the aconitase activity and the Aco1 content was shown. Results are means of three independent cultures, and the error bars indicate ± S.D. *P < 0.05; **P < 0.05, ***P < 0.01 (as assessed with the Newman-Keuls Multiple Comparison Test). The raw data corresponding to these results are available as supplementary information (Table S5).

Figure 6. Effect of *ACO1* overexpression on zinc tolerance of *pif1*Δ and *aco1*Δ mutants. (**A**) Aconitase activity and (**B**) Aco1 protein content were measured in BY4741, *aco1*Δ, *pif1*Δ mutants and *aco1*Δ, *pif1*Δ mutants transformed with pVT-U and pVT-U/*ACO1* plasmids. Cells were grown in minimal medium overnight at 30 ºC and diluted in fresh minimal medium to an OD_{600} of 0.1. They were subsequently grown to an OD_{600} ~0.4-0.6, then the cells were collected. The values shown are the mean of three independent cultures, and the error bars indicate ±1 S.D. **C.** BY4741, *aco1*Δ and *pif1*Δ were transformed with pVT-U/*ACO1* or the empty vector and all of them were grown in minimal medium overnight at 30 ºC and then diluted in fresh minimal medium to an OD_{600} of 0.1. Cultures were grown to an exponential phase (OD_{600} 0.3-0.5) and then were diluted and spotted into YPD, YPD + 5mM $ZnCl_2$. They were allowed to grow for 72h. Results are means of three independent cultures, and the error bars indicate ± S.D. Significance is shown regarding the BY4741 (wild type) strain values. *P < 0.05; **P < 0.05, ***P < 0.01 (as assessed with the Newman-Keuls Multiple Comparison Test). The raw data corresponding to these results are available as supplementary information (Table S6).

Figure 7. Measurements of the citrate content in the different *aco1* and *pif1*Δ mutants. Citrate content was measured from 60 absorbance units of cells in mid-log phase and early-stationary phase. Cultures were grown in YPD medium overnight at 30 ºC and then diluted in fresh YPD medium to an OD_{600} of 0.1 and they were grown to an exponential phase (OD_{600} 0.3-0.5), when samples were collected and frozen at -80 ºC. Results are means of three independent cultures, and

the error bars indicate ± S.D. Significance is shown regarding the BY4741 (wild type) strain values. *P < 0.05; **P < 0.05, ***P < 0.01 (as assessed with the Newman-Keuls Multiple Comparison Test). The raw data corresponding to these results are available as supplementary information (Table S7).

Figure 8. Intracellular and mitochondrial iron and zinc content measurements. Cells were grown in YPD medium overnight at 30 ºC and diluted in fresh YPD medium to an OD_{600} of 0.1, then growth was allowed until to an OD_{600} ~0.4 and (t_0, grey bars). The culture was divided into two parts, and one of them was supplemented with 5 mM $ZnCl_2$. Both cultures were grown for 24 hours and t_{24} (white bars) and t_{24+Zn} (black bars) and then cells were collected. **A**. Total and (**B**) mitochondrial zinc levels in different strains were shown. **C**. Total and (**D**) mitochondrial iron levels in different strains were shown. Results are means of three independent cultures, and the error bars indicate ± S.D. Significance is shown regarding the BY4741 (wild type) strain values. *P < 0.05; **P < 0.05, ***P < 0.01 (as assessed with the Newman-Keuls Multiple Comparison Test). The raw data corresponding to these results are available as supplementary information (Table S8).

Figure 9. Semi-quantitative RT-PCR of iron metabolism related genes in wild type, *aco1*Δ and *pif1*Δ strains. mRNA levels of different genes whose products are involved in iron transport were analysed by semi-quantitative RT-PCR, using *ACT1* for normalization. **A**. Cells were grown in YPD medium overnight at 30 ºC and diluted in fresh YPD medium to an OD_{600} of 0.1, and they were subsequently allowed to reach an OD_{600} ~0.4 for exponentially growing samples. **B**. The culture was allowed to grow until OD_{600} ~2 and the early stationary phase samples were collected One representative set of the triplicates of the experiment is shown.

Figure 10. Succinate dehydrogenase activity measurements. The succinate dehydrogenase activity was measured in the wild type strain, *aco1* and *pif1*Δ mutants, relative to BT-formazan salts formation. Cells were grown in YPD medium overnight at 30 ºC and diluted in fresh YPD medium to an OD_{600} of 0.1, then growth was allowed until to an OD_{600} ~0.4 and then were collected. The experiment was carried out as explain in Material and Methods section. Results are means of three independent cultures, and the error bars indicate ± S.D. Significance is shown regarding the BY4741 (wild type) strain values. *P < 0.05; **P < 0.05, ***P < 0.01 (as assessed with the Newman-Keuls Multiple Comparison Test). The raw data corresponding to these results are available as supplementary information (Table S9).

REFERENCES

1 J. De Freitas, H. Wintz, J. Kim, H. Poynton, T. Fox, and C. Vulpe, *Biometals*, 2003, **16**, 185-197.

2 M. R. Bleackley and R. T. Macgillivray, *Biometals,* 2011, **24**, 785-809.

3 C. Andreini, I. Bertini and A. Rosato, *Bioinformatics,* 2004, **20,** 1373-1380.

4 D. J. Eide, *J. Biol. Chem.,* 2009, **284**, 18565-18569.

5 M. Guirola, L. Barreto, A. Pagani, M. Romagosa, A. Casamayor, S. Atrian, and J. Ariño, *Biochem. J.*, 2010, **432**, 595-605.

6 A. Pagani, A. Casamayor, R. Serrano, S. Atrian and J. Ariño, *Mol. Microbiol.,* 2007*,* **65**, 521-537.

7 T. A. Rouault, *Nat. Chem. Biol.,* 2006, **2,** 406-414.

8 X. J. Chen, X.Wang, B. A. Kaufman and R. A. Buttow, *Science,* 2005*,* **307**, 714-717.

9 B. A. Kaufman, S. M. Newman, R. L. Hallberg, C. A. Slaughter, P. S. Perlman and R. A. Buttow, *Proc. Natl. Acad. Sci. USA,* 2000, **97**, 7772-7777.

10 X. J. Chen and R. A. Buttow, *Nat. Rev. Genet.,* 2005*,* **6**, 815-825.

11 X. J. Chen, X.Wang and R. A. Buttow, *Proc. Natl. Acad. Sci. USA,* 2007*,* **104**, 13738-13743.

12 T. Vernet, D. Dignard and D. Y. Thomas, *Gene,* 1987*,* **52**, 225-233.

13 R. S. Sikorski and P. Hieter, *Genetics,* 1989*,* **122**, 19-27.

14 R. D. Gietz, A. St.Jean, R. A. Woods and R. H. Schiestl, *Nucleic Acids Res.,* 1992, **220**, 1425.

15 G. Bellí, E. Garí, L. Piedrafita, M. Aldea and E. Herrero, *Nucleic Acids Res*., 1998*,* **26**, 942-947.

16 M. S. Longtine, A. Mckenzie III, D. J. Demarini, N. G. Shah, A. Wach, A. Brachat, P. Philippsen and J. R. Pringle, *Yeast*, 1998, **14**, 953-961.

17 B. Fansler and J. M. Lowenstein, *Methods Enzymol*., 1969, **13**, 26-30.

18 J. B. J. Robinson, L. G. Brent, B. Sumegi and P. A. Srere, in *Mitochondria, a Practical Approach*, eds. W. M. Darley-Usmar, D. Richwood and M. T. Wilson, IRL press, Oxford, 1987, pp. 153-170.

19 A. Lin, K. W. Kahala, S. T. Weintraub and L. McAlister-Henn, *Arch. Biochem. Biophys.,* 2008*,* **474**, 205-212.

20 O. S. Chen, S. Hemenway and J. Kaplan, *Proc. Natl. Acad. Sci. USA.,* 2002, **99**, 16922-16927.

21 D. Kregiel, J. Berlowska and W. Ambroziak, *Food Technol. Biotechnol*., 2008, **46**, 376-380.

22 K. Juneau, M. Miranda, M. E. Hillenmeyer, C. Nislow and R. W. Davis, *Genetics,* 2006, **174**, 511-518.

23 A. Ståhlberg, K. Elbing, J. M. Andrade-Garda, B. Sjögreen, A. Forootan and M. Kubista, *BMC Genomics,* 2008, **9**, 170-185.

24 L. Zheng, M. C. Kennedy, H. Beinert and H. Zalkin, *J. Biol. Chem.,* 1992, **267**, 7895-7903.

25 A. H. Robbins and C. D. Stout, *Proc. Natl. Acad. Sci. USA.,* 1989, **86**, 3639-3643.

26 R. Ben-Menachem, N. Regev-Rudzki and O. Pines, *J. Mol. Biol.,* 2011, **409**, 113-123.

27 L. C. Costello, Y. Liu, R. B. Franklin and M. C. Kennedy, *J. Biol. Chem*., 1997, **272**, 28875-28881.

28 W. H. Tong and T. A. Rouault, *Biometals*, 2007, **20**, 549-564.

29 C. C. Philpott and O. Protchenko, *Eukaryot. Cell,* 2008, **7**, 20-27.

30 Y. Yamaguchi-Iwai, R. Ueta, A. Fukunaka and R. Sasaki, *J. Biol. Chem*., 2002, **277**, 18914-18918.

31 O. S. Chen, R. J. Crisp, M. Valachovic, M. Bard, D. R. Winge and J. Kaplan, *J. Biol. Chem*., 2004, **279**, 29513-29518.

32 J. C. Rutherford, L. Ojeda, J. Balk, U. Mühlenhoff, R. Lill and D. R. Winge, *J. Biol. Chem*., 2005, **280**, 10135-10140.

33 C. J. Frederickson, J. Y. Koh and A. I. Bush, *Nat. Rev. Neurosc.,* 2005*,* **6**, 449-462.

34 M. Holz, A. Förster, S. Mauersberger and G. Barth, *Appl. Microbiol. Biotechnol.,* 2009*,* **81**, 1087-1096.

35. R. B. Martin, *J. Inorg. Biochem.,* 1986, **28**, 181-187.

36 J. L. Pierre and I. Gautier-Luneau, *Biometals,* 2000, **13**, 91-96.

37 H. Glickstein, R. B. Ben-El, M. Shvartsman and Z. I. Cabantchik, *Blood,* 2005, **106**, 3242–3250.

38 H. Glickstein, R. B. Ben-El, G. Link, W. Breuer, A. M. Konijn, C. Hershko, H. Nick and Z. I. Cabantchik, *Blood,* 2006, **108**, 3195–3203.

39 W. Breuer, M. Shvartsman and Z. I. Cabantchik, *Int. J. Biochem. Cell. Biol.,* 2008, **40,** 350-354.

40 K. K. Singh, M. M. Desouki, R. B. Franklin and L. C. Costello, *Mol. Cancer*, 2006, **5**, 14.

41 L. C. Costello and R. B. Franklin, *Mol. Cancer*, 2006, **5**, 17.

42 V. Kolenko, E. Teper, A.Kutikov and R. Uzo, *Nat. Rev. Urol.,* 2013, **10**, 219-226.

43 K. Kitamoto, K. Yoshizawa, Y. Ohsumi and Y.Anraku, *J. Bacteriol*., 1988, **170**, 2683-2686.

44 C. Simm, B. Lahner, D. Salt, A. Le Furgey, P. Ingram, B. Yandell and D. Eide, *Eukaryot. Cell,* 2007*,* **6**, 1166-1177.

45 C. C. Philpott, R. D. Klausner and T. A. Rouault, *Proc. Natl. Acad. Sci. USA,* 1994, **91**, 7321-7325.

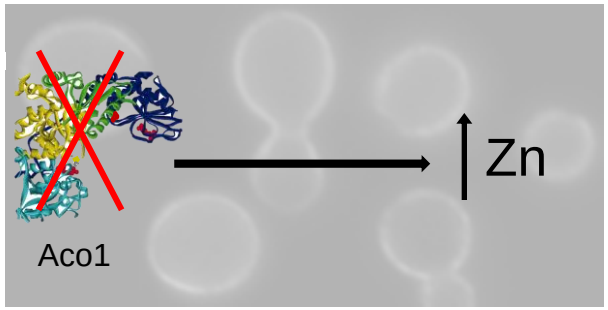

In yeast, the lack of mitochondrial aconitase activity determines high-zinc tolerance, which is accompanied by the alteration of several low-iron sensor signals.

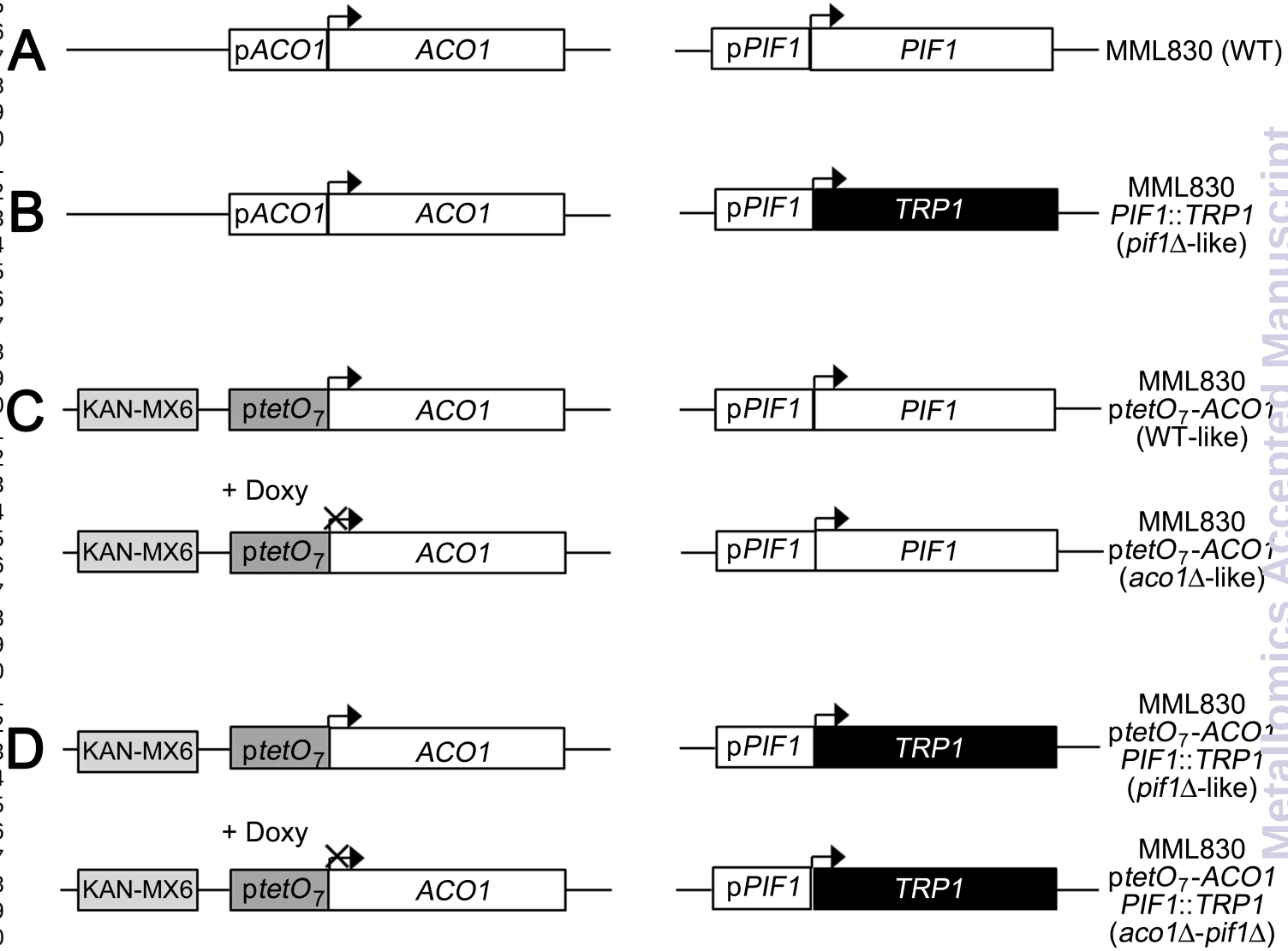

Fig. 1

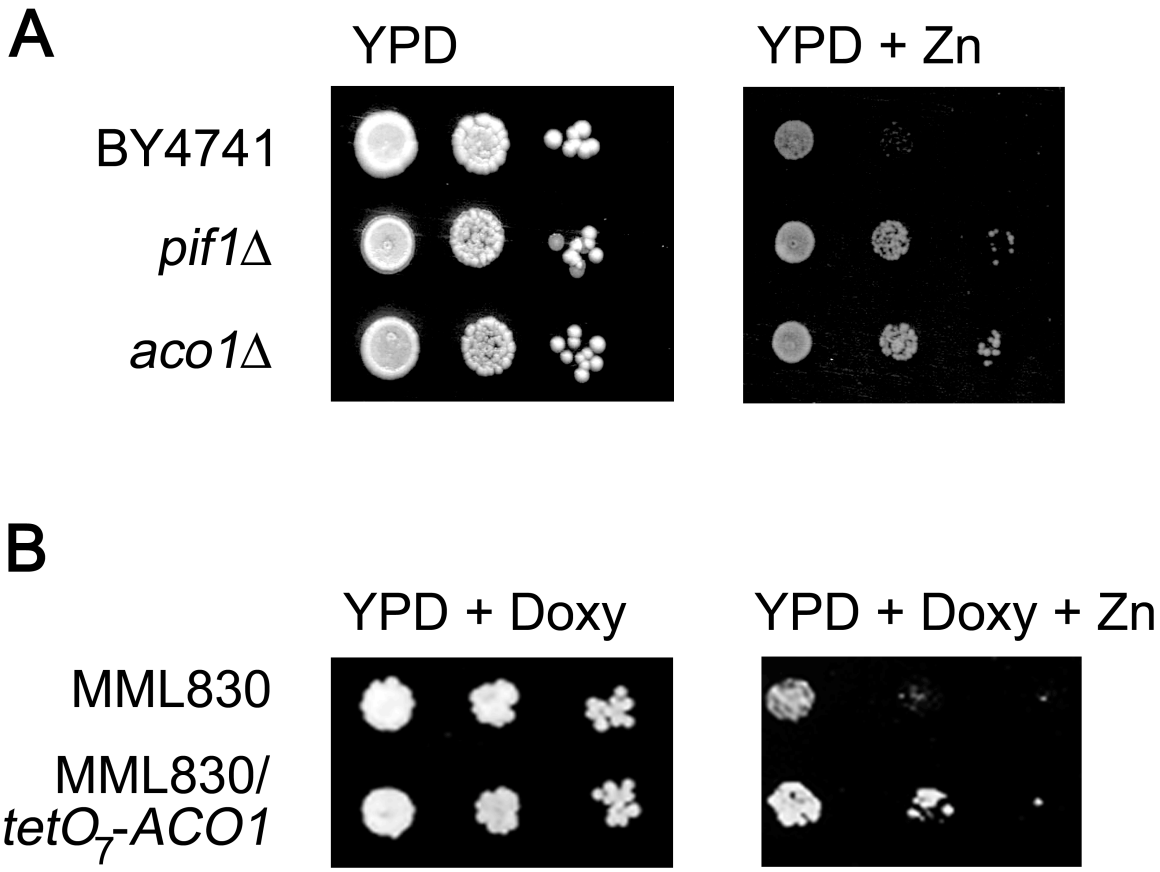

Fig. 2

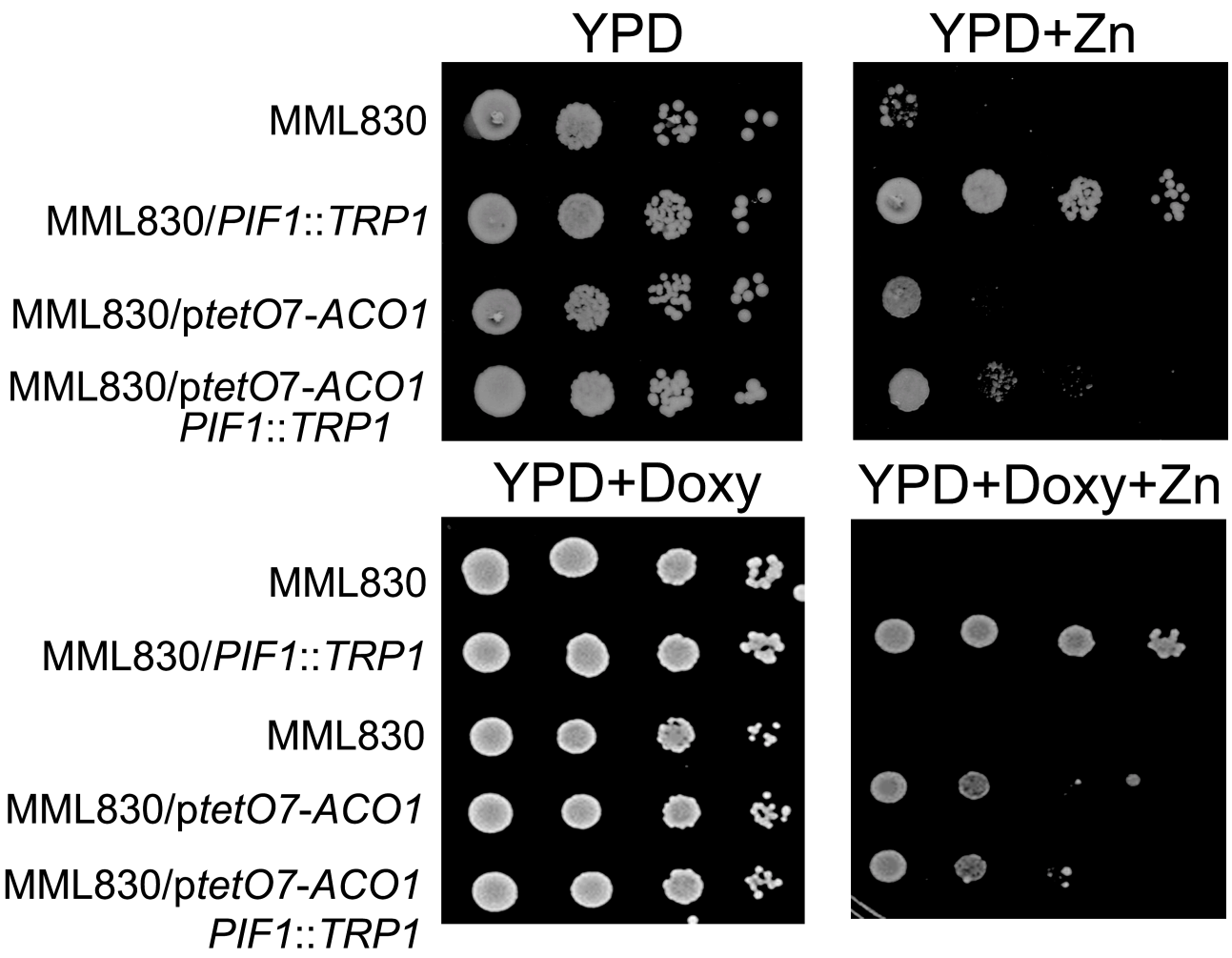

Fig. 3

	Enzymatic activity	*In vivo* DNA-binding capacity	*In vivo* mtDNA maintenance
BY4741	100%	100%	+
*aco1*Δ	-	-	-
aco1–Δd4	-	10%	-
aco1-C448S	-	100%	+
aco1-R476S	75%	50%	-
aco1-R668S	87%	20%	-

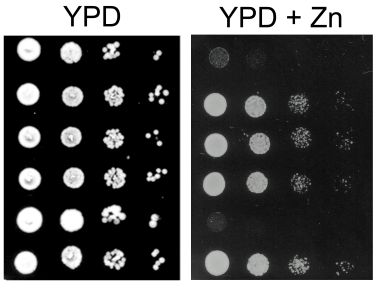

Fig. 4

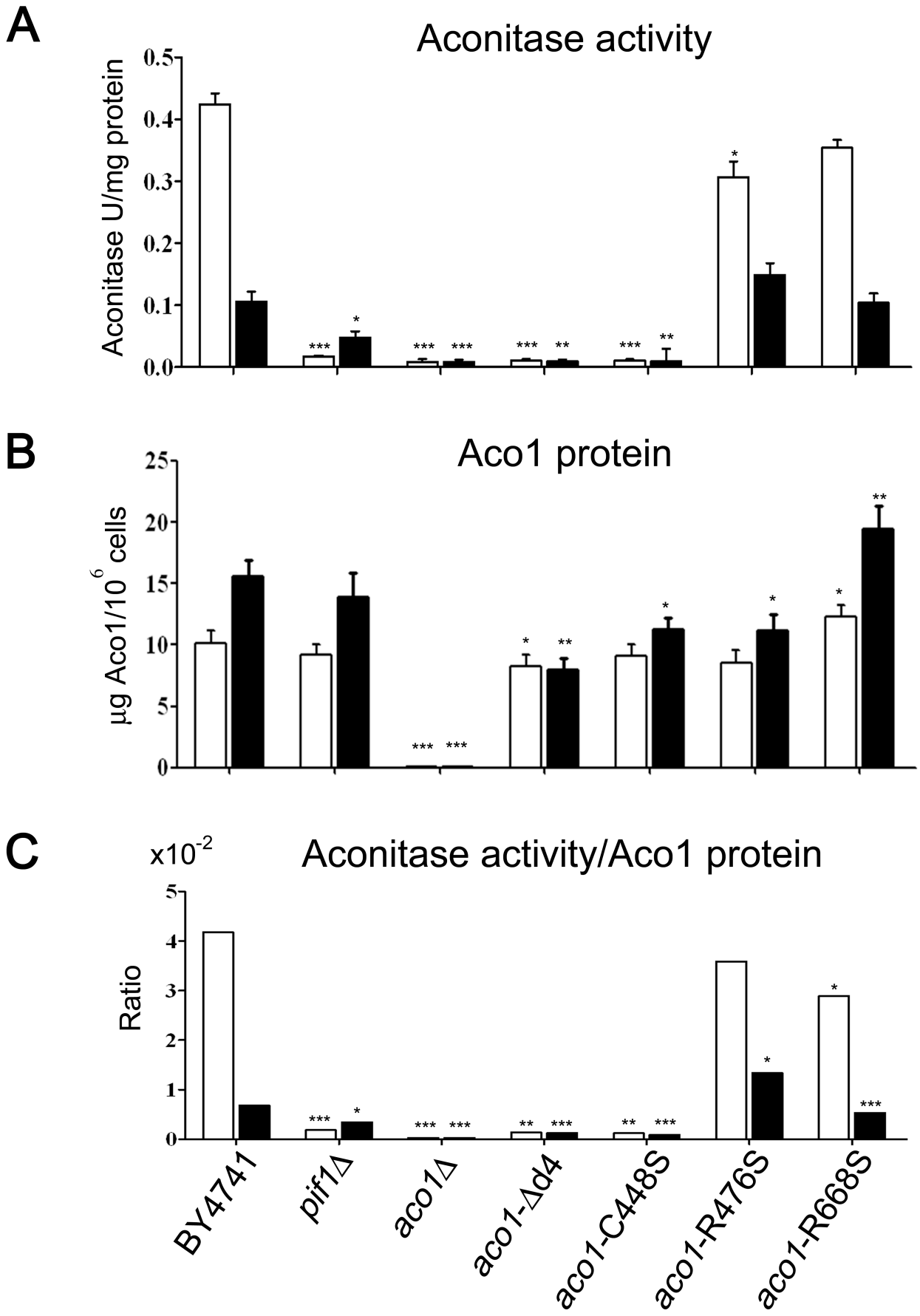

Fig. 5

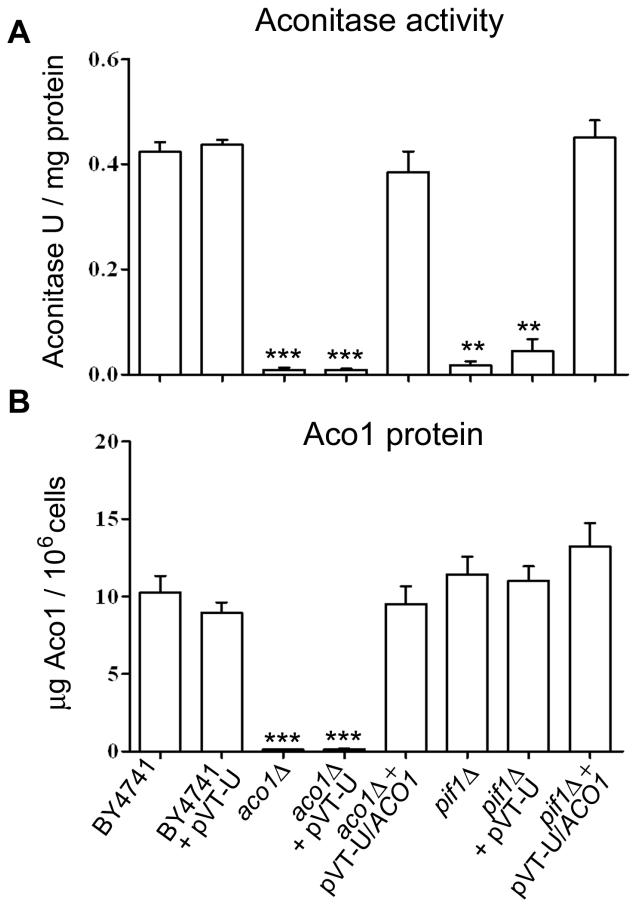

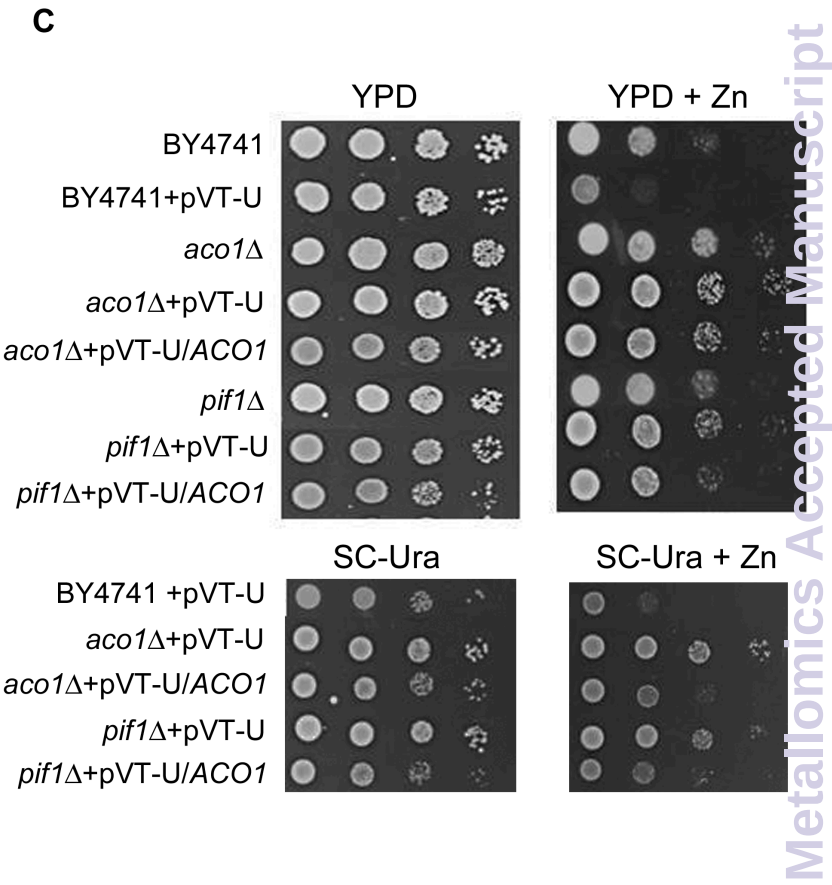

Fig. 6

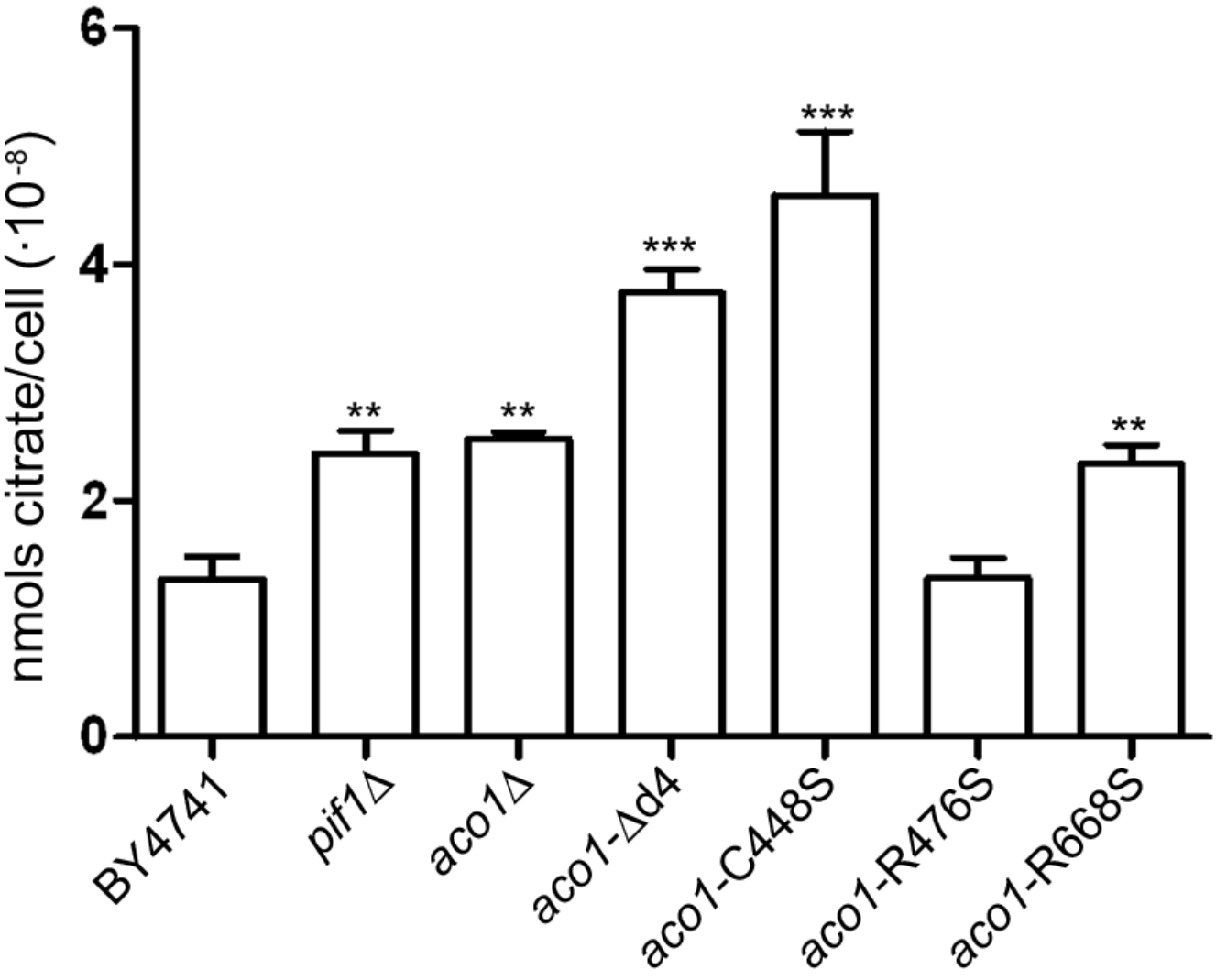

Fig. 7

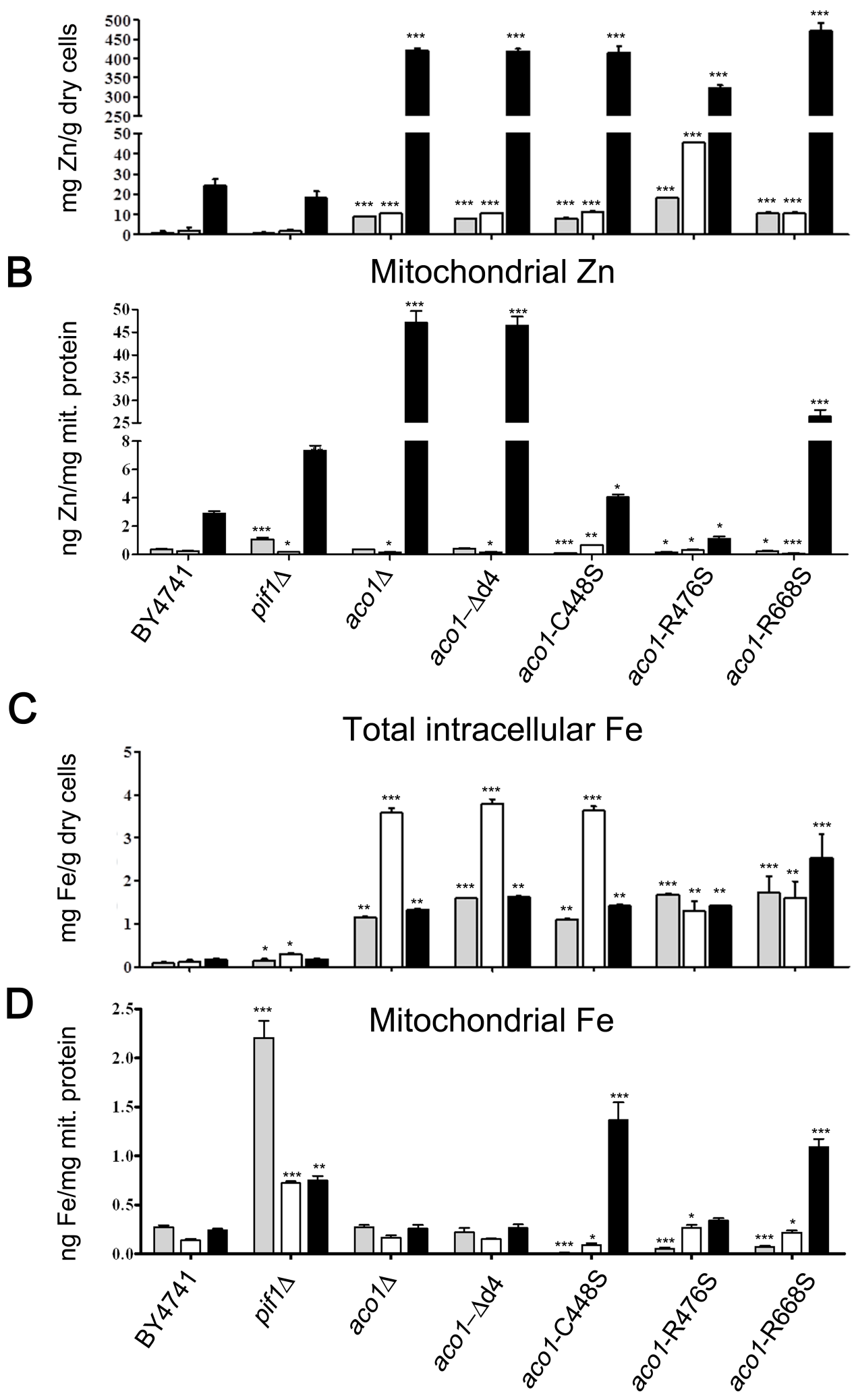

Fig. 8

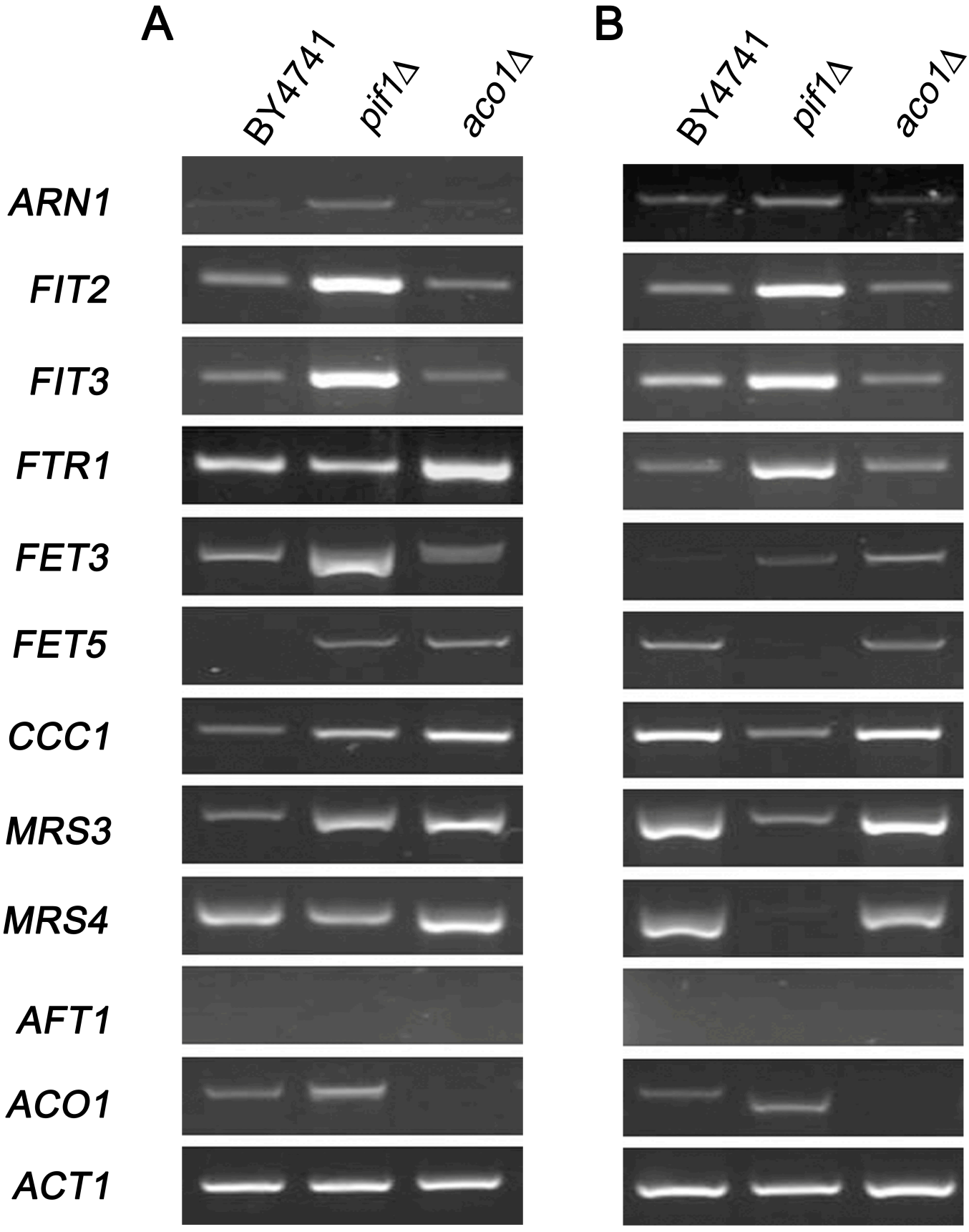

Fig. 9

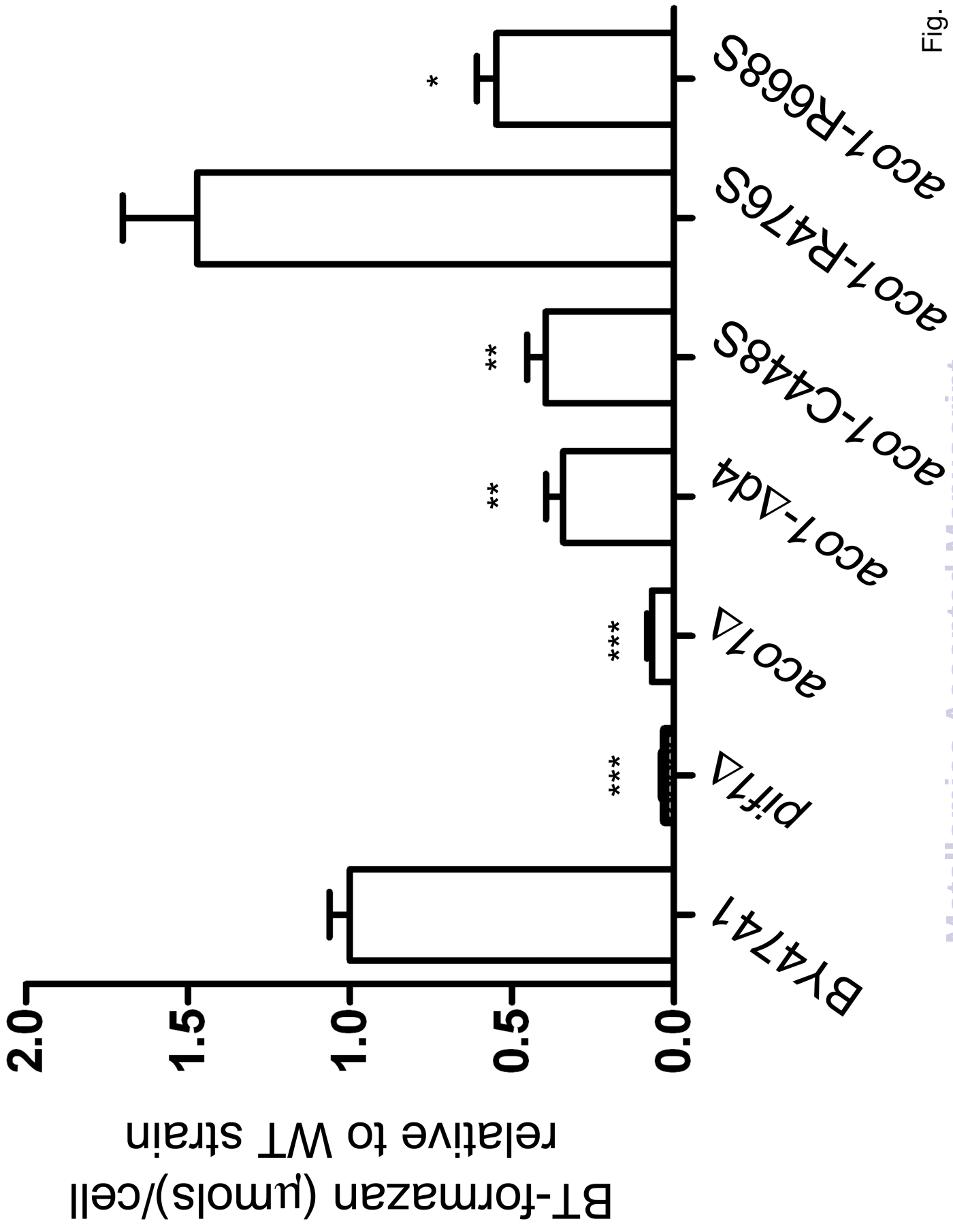

Fig. 10